Journal of Crohn's and Colitis, 2022, 656–667
https://doi.org/10.1093/ecco-jcc/jjab179
Advance Access publication October 10, 2021
Original Article

Original Article

MiR-1-3p and MiR-124-3p Synergistically Damage the Intestinal Barrier in the Ageing Colon

Ting-yi Sun,[a,b,c,*] Ya-qi Li,[a] Fu-qian Zhao,[a] Hai-mei Sun,[a,b,c] Yang Gao,[a] Bo Wu,[a,b,c] Shu Yang,[a,b,c] Feng-qing Ji,[a,b,c,*] De-shan Zhou[a,b,c,*]

[a]Department of Histology and Embryology, School of Basic Medical Sciences, Capital Medical University, Beijing, China [b]Research Lab of Gastrointestinal Tract Histopathology, Beijing Key Laboratory of Cancer Invasion and Metastasis Research, Beijing, China [c]Research Lab of Gastrointestinal Tract Histopathology, Cancer Institute of Capital Medical University, Beijing, China

*These authors contributed equally to this article.

Corresponding author: De-shan Zhou, PhD, Department of Histology and Embryology, School of Basic Medical Sciences, Capital Medical University, Beijing 100069, China. Fax and tel.: +86-10-83950491; email: zhouds08@ccmu.edu.cn

Abstract

Background and Aims: Disruption of the intestinal barrier of the digestive tract is a common pathophysiological change in the elderly, which may partly contribute to gut dysfunction and inflammatory bowel disease [IBD]. This study aimed to discover new interactive epigenetic regulation patterns involved in intestinal barrier dysfunction and colitis in elderly populations.

Methods: Intestinal barrier function and structure were evaluated in naturally ageing mice and elderly people. High-throughput analysis was performed on colonic tissues from humans and mice. The synergistic roles of *miR-1-3p* and *miR-124-3p* were identified using microRNA mimic/agomirs. Related genes were examined in biopsies of old IBD patients.

Results: A defective mucus barrier was observed before mucosal microstructural damage during ageing. Elevated *miR-1-3p* expression in the colons of older individuals impaired the mucus barrier by directly targeting T-synthase, similarly to the mechanism of *miR-124-3p*, which we reported previously. Importantly, the synergistic effect of a half dose of each microRNA supplement on T-synthase and CDK4/6 was stronger than that of a full dose of *miR-1-3p* or *miR-124-3p* alone, and mice co-treated with two microRNAs showed greater susceptibility to chemical-induced colitis than mice treated with either microRNA alone. These two microRNAs were up-expressed in old IBD patients.

Conclusions: The slight increases in *miR-1-3p* and *miR-124-3p* expression with ageing may be important contributors to the breakdown of intestinal homeostasis by targeting divergent genes in different cells. These data reveal the potential ability of multiple microRNAs to exert synergistic effects to damage the intestinal barrier and promote inflammatory bowel disease development in elderly populations.

Graphical Abstract

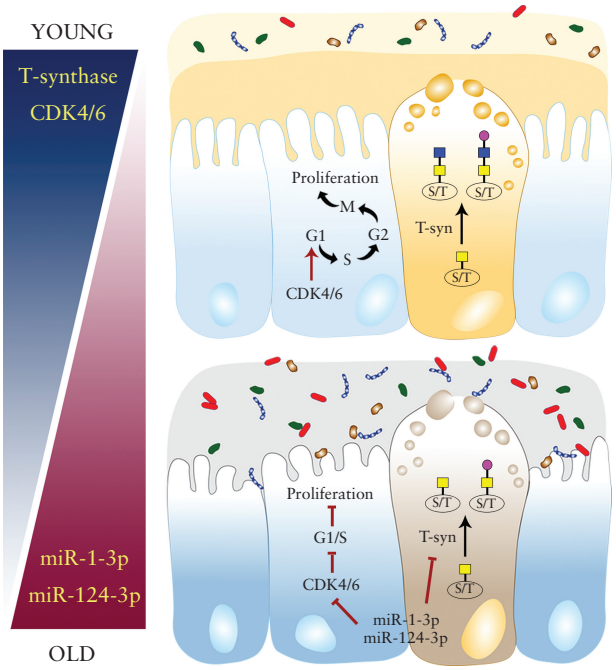

Keywords: Intestinal barrier; ageing; synergy

1. Introduction

Inflammatory bowel disease [IBD], which includes ulcerative colitis [UC] and Crohn's disease [CD], is a group of chronic, recurrent, incurable intestinal diseases that cause severe inflammation and ulceration of the gastrointestinal [GI] tract. As the global prevalence of IBD has continued to increase in recent years, IBD has imposed a significant financial and resource burden on health care systems.[1,2] With the rapid increase in the ageing population throughout the world [according to the United Nations 2019 Revision of World Population Prospects], the elderly population is the fastest-growing subpopulation of people with IBD, due to both the ageing of previously diagnosed patients and the diagnosis of new cases in this subpopulation.[3,4] Elucidating the precise aetiology of GI inflammation, particularly in IBD, in elderly populations is important for addressing the challenge of treating the increased number of ageing patients and to help achieve gradual healthy ageing.

IBD is a multifactorial disease involving host genetic susceptibility, environmental triggers, immune dysregulation, and altered intestinal microbiota homeostasis, the last of which is partly influenced by dynamic cross-talk between the gut microbiota and intestinal barrier.[5,6] Generally, the normal intestinal barrier consists of multiple layers, including: [1] the micro-ecological barrier; [2] the mucus gel layer; [3] intestinal epithelial cells [IECs] that form a single-cell layer of physical protection; and [4] the immune barrier.[7] Accumulating experimental evidence indicates a crucial role of intestinal barrier dysfunction in the onset of IBD, suggesting that such dysfunction is a potential predisposing factor for IBD.[8,9] As one of the hallmarks of health,[10] the intestinal barrier is progressively damaged during senescence.[11] Our recent work[12] demonstrated that age-related changes in mucus properties increase the susceptibility to colitis in elderly populations. However, research on the underlying regulatory mechanism is far from comprehensive.

Broadly, microRNAs [miRNAs] are believed to be among the key molecular regulators of gut homeostasis. Abnormal miRNA expression and function appear to be pervasive features of almost all related diseases.[13,14] Evidence regarding the mechanisms by which specific miRNAs control the progression of digestive tract inflammation and tumour has emerged from many studies, showing that the concerted targeting of multiple genes by a single miRNA is responsible for dramatic effects. However, the interaction and mode of action of different miRNAs in GI diseases remain unclear. Here, we identified a set of miRNAs, *miR-1-3p* and *miR-124-3p*, whose expression was mildly upregulated in the ageing distal colonic mucosa. These miRNAs convergently target T-synthase and cyclin-dependent kinase [CDK] 4 and CDK6, and comprise a cooperative miRNA network that impairs intestinal barrier integrity. Our study may provide new research targets for both delaying GI senescence and ameliorating IBD symptoms.

2. Materials and Methods

2.1. Animals

Male C57BL/6 mice were purchased from Capital Medical University and divided into three groups of 10 each according to age, i.e., 2, 16, and 24 months [mo], to simulate the life phases at approximately 20, 50, and 70 years of age in humans.[15] An additional 30 male mice [aged 2 mo] were used to establish the *miR-1-3p* agomir treatment model [n = 5 per group] and the dextran sulphate sodium [DSS]-induced colitis model [n = 5 per group]. All mice were housed in a controlled environment under a 12-h light/dark cycle at 22 ± 2 ℃ and 55 ± 5% humidity, with *ad libitum* access to food and water, and were sacrificed by appropriate anaesthesia and/or cervical dislocation before sample collection. Colon and liver tissues were surgically and aseptically removed from

the mice. All animal procedures were carried out under protocols approved by the Animal Care and Use Committee of Capital Medical University [Permit Number AEEI-2016-143, 17 October 2016].

2.2. Human tissue samples

A total of 14 normal mucosal tissue samples were collected from colorectal cancer patients immediately after surgical resection at Beijing Friendship Hospital, Capital Medical University [Beijing, China]. All patients met the following inclusion criteria: [1] age: young adults <45 years [*n* = 7, 27 to 44 years, 4 males and 3 females] and elderly adults >70 years [*n* = 7, 72 to 81 years, 5 males and 2 females]; [2] all patients were chemotherapy- and radiation therapy-naïve; and [3] normal tissue samples were harvested from the descending colon [distal colon]. The distal colonic mucosal biopsy specimens were obtained from patients with clinically active IBD including 13 patients with UC and one patient with CD. All patients divided into two groups according to age: young IBD patients <37 years [*n* = 5, 29 to 37 years, 2 males and 3 females, 5 patients with UC]; and elderly IBD patients >73 years [*n* = 9, 73 to 81 years, 6 males and 3 females, 8 patients with UC and 1 patient with CD]. A diagnosis of IBD was defined by clinical, radiological, endoscopic, and histological criteria. None of the patients received antibiotics, steroids, or immunosuppressive agents. The protocol for human biospecimen collection was approved by the Clinical Research Ethics Committee of Beijing Friendship Hospital, Capital Medical University [Permit Number 2015SY12, 9 March 2015]. After collection, the samples were stored at -80°C.

2.3. Administration of *miR-1-3p* agomir

Young [aged 2 mo] mice were randomly assigned to two groups [*n* = 5 per group] and injected via tail vein with either micrON *miR-1-3p* agomir [5'-UGGAAUGUAAAGAAGUAUGUAU-3', Cat. No.miR40000416-4-5, RiboBio, China] or micrON agomir negative control [NC, Cat.No.miR4N0000001-4-5, RiboBio, China] at a dose of 8 nmol/day on 2 consecutive days. The mice were sacrificed 96 h after the last injection, and tissues were collected for further analyses [Supplementary Figure 1A, available as Supplementary data at *ECCO-JCC* online].

2.4. DSS-induced colitis model

The procedure used to generate the DSS colitis model is shown in Supplementary Figure 1A. Our published data[12] demonstrated that *miR-1-3p* expression in the distal colon mucosa of 24-mo-old mice was 1.6 times higher than that of *miR-124-3p*. These previous data provide a reference for the miRNA agomir dose required in the animal model. Four groups of young mice [aged 2 mo, *n* = 5 per group] received tail vein injections of: [1] *miR-1-3p* agomir [8 nmol/day]; [2] *miR-124-3p* agomir [5 nmol/day, 5'-UAAGGCACGCGGUGAAUGCC-3', Cat.No.miR40000134-4-5, RiboBio, China]; [3] *miR-1-3p* agomir [4 nmol/day] combined with *miR-124-3p* agomir [2.5 nmol/day]; and [4] agomir NC [8 nmol/day] on 2 consecutive days. This treatment regimen was applied once at a 4-day interval to maintain high miRNA expression. Simultaneously, acute colitis was induced by the continuous administration of 5% DSS [Cat.No.0216011080, MP Biomedicals, USA] in drinking water for 4 days, and the mice were euthanised on Day 8. Disease severity in the mice with DSS-induced colitis was assessed as we previously described.[12]

2.5. High-throughput analysis

2.5.1. MiRNA microarray analysis

Total RNA was isolated from human distal colon mucosal tissues using TRIzol reagent [Life Technologies, USA] and a miRNeasy mini kit [Qiagen, USA]. Biotinylated cDNA was prepared from 250 ng total RNA according to the standard Affymetrix protocol by using the Ambion® WT Expression Kit. After labelling, fragmented cDNA was hybridised for 16 h at 45℃ on a GeneChip ® miRNA 4.0 Array [Affymetrix]. The GeneChips were washed and stained in an Affymetrix Fluidics Station 450. All arrays were scanned by using an Affymetrix® GeneChip Command Console, which was installed in the GeneChip® Scanner 3000 7G. Data were analysed with the robust multichip analysis algorithm using Affymetrix default analysis settings, and values are presented as the $\log_2$ robust multichip analysis signal intensity. The microarray data are publicly available at NCBI Gene Expression Omnibus under accession number GSE174837.

2.5.2. MiRNA sequencing

Mouse distal colon mucosal tissues were sent to Shanghai Gminix, Biotechnology [Shanghai, China]. Total RNA was used as input material for the small RNA library. The sequencing library was generated using a TruSeq preparation kit [Illumina, San Diego, CA, USA]. The samples were sequenced on the Illumina HiSeq platform [Illumina], and 50-bp single-end reads were generated. Data were deposited in the Gene Expression Omnibus under accession number GSE175493.

2.6. Data analysis

Images were acquired with a fluorescence microscope [Nikon 80i, Japan] or light microscope [Leica DM LB2] and analysed using ImageJ 1.52a [National Institutes of Health, USA]. The numbers of alcian blue/periodic acid-Schiff [AB/PAS]-positive goblet cells, 5'-bromo-2'-deoxyuridine [BrdU]-positive cells, and Ki67-positive cells per crypt were quantified by counting the number of cells in intact, well-oriented crypts with visible adjacent nuclei and lumen. Ten colonic crypts per section and three random sections were counted per mouse, with five mice per group.

2.7. Statistical analysis

All quantitative data are presented as the mean ± standard deviation [SD]. We analysed the normality of the data distribution and homogeneity of variance using Shapiro-Wilk's and Levene's test, respectively. Statistical differences were analysed using Student's t test [parametric data] or Mann–Whitney U test [nonparametric data] for two groups and one-way analysis of variance [ANOVA] followed by LSD or Dunnett's T3 post hoc test for multiple groups. A *p*-value <0.05 was considered to indicate statistical significance. Statistical analysis was performed and data were plotted by SPSS 21.0 software [IBM Corp., Armonk, NY, USA] and GraphPad Prism 8 [GraphPad Software, San Diego, CA, USA].

2.8. Other methods

Please see the Supplementary experimental procedures [available as Supplementary data at *ECCO-JCC* online] for details regarding intestinal permeability assay, IEC proliferation, tissue preparation and staining, biotinylated lectin detection, fluorescence *in situ* hybridisation [FISH], cell culture, transfection of miRNA mimics, dual-luciferase reporter assay, cell counting kit-8 [CCK-8] assay, real-time monitoring of cell proliferation, western blot analysis, RNA and genomic DNA extraction and real-time polymerase chain reaction [PCR]. The antibodies and primers used are listed in Supplementary Tables 1 and 2, available as Supplementary data at *ECCO-JCC* online, respectively.

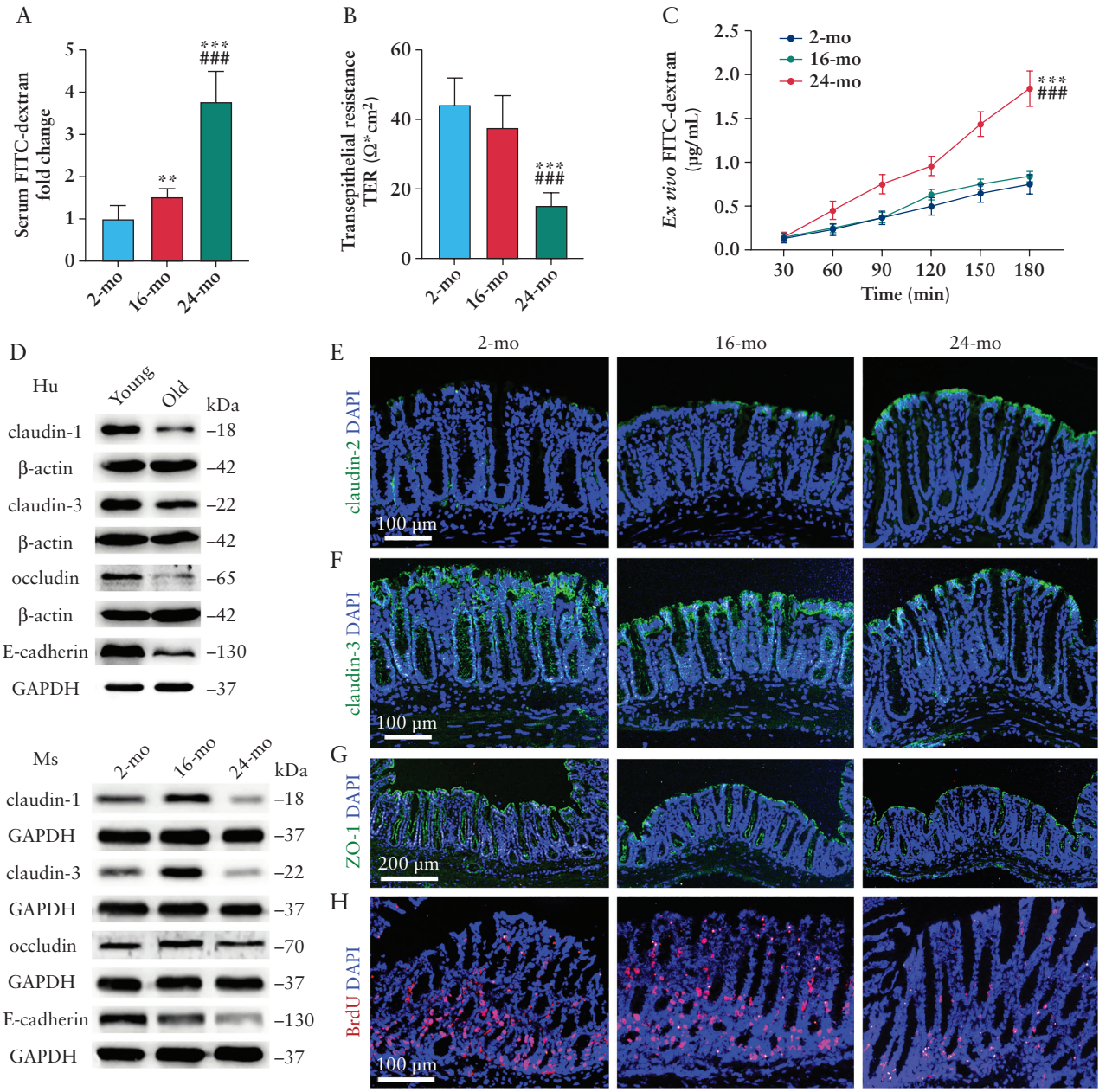

Figure 1. Colons exhibit impaired intestinal barrier integrity with age. A] Intestinal barrier dysfunction in 16- and 24-mo old mice detected by measuring serum FITC-dextran levels. B, C] Alterations in distal colonic TER [B] and *ex vivo* permeability [C] in 2-, 16-, and 24-mo old mice as detected by Ussing-chamber. D–G] Western blot analysis [D] and immunofluorescence images [E–G] showing lower expression of claudin-1, claudin-3, occludin, E-cadherin, and ZO-1 and higher expression of claudin-2 in distal colon mucosal tissues of 24-mo old mice and elderly people. H] Representative fluorescence images showing a decrease in the number of BrdU-positive cells in the distal colons of 24-mo old mice. Data are presented as mean ± SD; $^{**}p$ <0.01, $^{***}p$ <0.001 compared with 2-mo old mouse group; ###p <0.001 compared with 16-mo old mouse group. ANOVA and Dunnett's T3 test for [A]; ANOVA and LSD test for [B, C]. n = 10 mouse samples per group. Hu, human; Ms, mouse; mo, month; TER, transepithelial resistance; SD, standard deviation.

3. Results

3.1. Distal colons show hyperpermeability and impaired epithelial barrier integrity with age

Our previous data showed that the mouse colon exhibits age-related microbiota dysbiosis and a breached inner mucus layer.[12] In this study, we measured mouse gut permeability *in vivo* to further assess intestinal barrier function during ageing. The guts of mice aged 16 and 24 mo showed greater permeability to fluorescein isothiocyanate [FITC]-dextran [Figure 1A]. Considering that the epithelial barrier acts as a physical barrier, we compared the transepithelial resistance [TER] of *ex vivo* distal colons and paracellular permeability based on the luminal-to-serosal flux of FITC-dextran across distal colon segments from mice in different age groups. Mice aged 24 mo showed distinctly decreased TER [Figure 1B] and markedly increased permeability [Figure 1C]. Then, the architecture of mouse and human distal colons was examined by measuring the expression of intercellular junction proteins, such as claudin-1, claudin-2, claudin-3, occludin, zonula occludens-1 [ZO-1], and E-cadherin, by western blot analysis [Figure 1D; Supplementary Figure 1B, C] and/or immunofluorescence [Figure 1E, F, G; Supplementary Figure 1D, E, F]. Impaired mucosal microstructure was clearly observed in mice aged

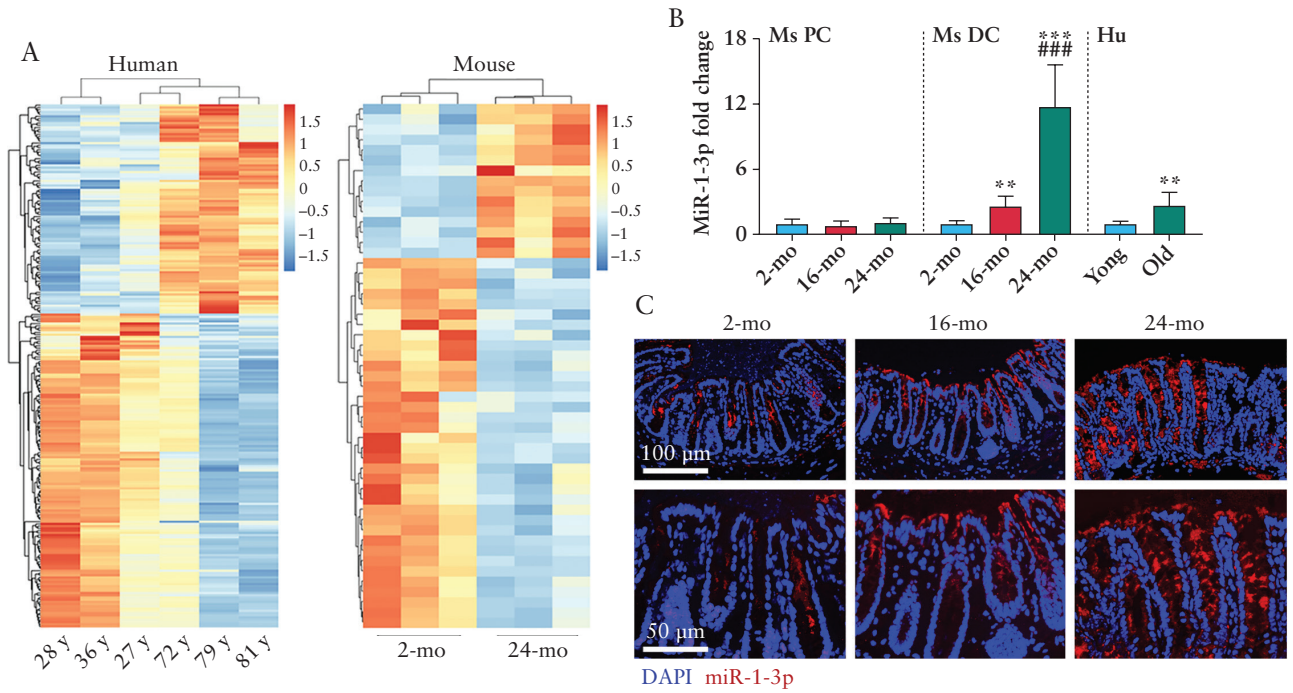

Figure 2. *MiR-1-3p* expression is upregulated in distal colons with age. A] Hierarchical clustering of the expression patterns of miRNAs differentially expressed in human and mouse distal colon mucosal tissues of the young and elderly groups. B] *MiR-1-3p* expression was higher in the distal colons of old mice and elderly humans. Data are presented as mean ± SD; $^{**}p$ <0.01, $^{***}p$ <0.001 compared with 2-mo old mouse group or young people group; $^{###}p$ <0.001 compared with 16-mo old mouse group. ANOVA and LSD test for [Ms PC]; ANOVA and Dunnett's T3 test for [Ms DC]; Student's t test for [Hu]. n = 10 mice or 7 human samples per group. C] Representative FISH images of the mouse distal colon showing higher expression of *miR-1-3p* with ageing. Ms, mouse; Hu, human; PC, proximal colon; DC, distal colon; SD, standard deviation; mo, month.

24 mo. We also found reduced numbers of BrdU- and Ki67-positive cells within the crypts in aged mice [Figure 1H; Supplementary Figure 1G, H, I], indicating that intestinal hyperpermeability in the colons of 24-mo old mice might partly be induced by mucosal microstructural damage and reduced epithelial self-renewal. Intriguingly, changes in intestinal epithelial microstructure appeared at 24 mo, but changes in mucus properties were observed beginning at 16 mo in the distal colon,[12] suggesting that changes in colonic mucus properties occur before those in intestinal microstructure.

3.2. *MiR-1-3p* expression is upregulated in the distal colon with age

Given that miRNA molecules are dysregulated in many diseases, miRNA expression in the normal distal colon mucosa from young and old humans and mice was determined by miRNA microarray analysis and miRNA sequencing, respectively. We identified 235 human miRNAs [p <0.05, Fold Change (FC) >2] and 51 mouse miRNAs [p <0.05, $|\log_2 FC|$ >0.6] that were differentially expressed between the young and old groups in Affymetrix miRNA Array dataset GSE174837 [*Homo sapiens*] and Illumina HiSeq dataset GSE175493 [*Mus musculus*], respectively. A heat map depicting the hierarchical clustering analysis is shown in Figure 2A. Five miRNAs [*miR-29c-3p*, *miR-1-3p*, *miR-378d*, *miR-133a-3p*, and *miR-490-3p*] had similar expression patterns in both humans and mice. Our previous study[12] found that T-synthase, the rate-limiting enzyme in mucin-type O-glycosylation, displays an age-related decline in expression. We integrated these five miRNAs and eight miRNAs predicted to regulate the T-synthase gene *C1GALT1* in the public databases PicTar, TargetScan, and miRanda[12] and obtained one specific miRNA, *miR-1-3p*. We further showed that *miR-1-3p* expression in the distal colonic mucosa was significantly increased in old mice and elderly persons, but no noticeable differences were observed in the proximal colonic mucosa [Figure 2B, C; Supplementary Figure 2, available as Supplementary data at *ECCO-JCC* online], indicative of a distinct regional expression pattern and trend opposite to that of T-synthase in the distal colon.[12] Thus, further experiments in this study focused on *miR-1-3p*.

3.3. Distal colons exhibit a loss of *O*-glycans with age, and *miR-1-3p* directly downregulates T-synthase expression

The lectin peanut agglutinin [PNA], which has a strong binding affinity for the T antigen, and *Vicia villosa* lectin [VVL], which preferentially recognises a single α-N-acetylgalactosamine residue linked to serine or threonine in the Tn antigen, were used for monitoring *O*-glycosylation. Fluorescence analysis of PNA and VVL in the mouse distal colon demonstrated the loss of T antigen and an abundance of Tn/sTn antigens in the 16- and 24-mo groups compared with the 2-mo group [Figure 3A; Supplementary Figure 3A, B, available as Supplementary data at *ECCO-JCC* online], indicating that abnormal colonic mucus properties were induced by mucin *O*-glycosylation deficiency. Given the age-related changes in *miR-1-3p* and T-synthase expression and the predicted relationship between these molecules, the 3' untranslated region [3'UTR] of *C1GALT1* was searched for potential *miR-1* binding sites using the TargetScan prediction algorithm [http://www.targetscan.org/vert_72/]. One possible binding site was identified, and to verify the binding site, we designed recombinant plasmids harbouring the wild-type or mutant *C1GALT1* 3'UTR sequences [Figure 3B; Supplementary Figure 3C, D]. Dual-luciferase reporter assay results indicated that *miR-1-3p* can bind

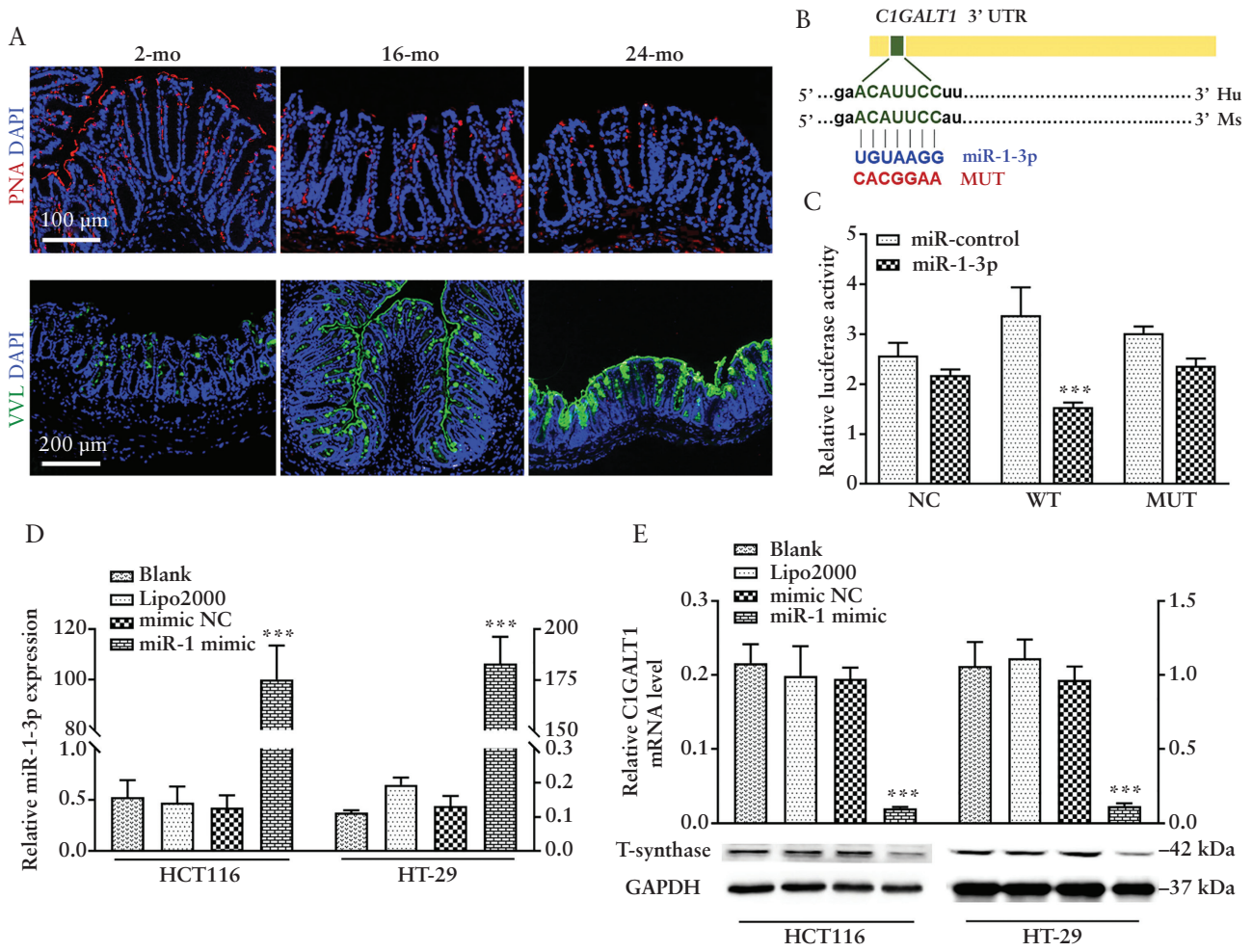

Figure 3. Distal colons show impaired mucus barrier integrity with age, and *miR-1-3p* downregulates T-synthase expression. A] Representative fluorescence images showing T antigen and Tn/sTn antigen expression by PNA and VVL staining in the distal colons of 2-, 16-, and 24-mo old mice. B] The predicted *miR-1-3p*-binding site and mutated binding site in the 3'UTR of the T-synthase gene *C1GALT1*. C] The results of the dual-luciferase reporter assay conducted in the 293T cell transfected with luciferase reporter constructs harbouring the wild-type [WT] or mutant [MUT] 3'UTR. Data are presented as mean ± SD. ***p <0.001 compared with miR-control group [ANOVA and LSD test]. n = 3 repeats. D] Real-time qPCR analysis of *miR-1-3p* expression in cells transfected with *miR-1-3p* mimic and NC. E] Low *C1GALT1* expression and T-synthase protein expression in cells transfected with *miR-1-3p* mimic. Data are presented as mean ± SD; ***p <0.001 compared with mimic NC group [ANOVA and LSD test]. n = 3 per group. SD, standard deviation; mo, month; NC, negative control.

to the 3'UTR of *C1GALT1* [Figure 3C]. Western blot analysis and real-time quantitative [q]PCR demonstrated that *miR-1-3p* directly downregulated the mRNA and protein expression of *C1GALT1* [Figure 3D, E; Supplementary Figure 3E].

3.4. Overexpression of *miR-1-3p* inhibits *O*-glycosylation, and *miR-1-3p* and *miR-124-3p* have a synergistic inhibitory effect on T-synthase expression

To determine whether increased *miR-1-3p* expression leads to the loss of T-synthase in the intestinal epithelium and causes defective mucus layer integrity, *miR-1-3p* agomir was administered to 2-mo old mice via intravenous injection into the tail vein [Supplementary Figure 1A]. Reduced T-synthase and *C1GALT1* levels were observed in both the proximal and distal colonic mucosa in agomir-treated mice compared with control mice [Figure 4A, B; Supplementary Figure 4A, available as Supplementary data at *ECCO-JCC* online], providing evidence that *C1GALT1* is a direct target gene of *miR-1-3p*. In addition to efficiently downregulating T-synthase expression, *O*-glycans were specifically depleted after treatment with the *miR-1-3p* agomir, as evidenced by Tn/sTn antigen deposition [Figure 4C; Supplementary Figure 4B, C] and abnormal *Ulex europaeus* agglutinin 1 [UEA1] staining [Figure 4D; Supplementary Figure 4D]. The gain of *miR-1-3p* led to the loss of *O*-glycans rather than a change in mucus secretion, because the thickness of the AB/PAS-positive mucus layer and the number of goblet cells remained unaltered in *miR-1-3p* agomir-treated mice [Figure 4E; Supplementary Figure 4E, F]. As expected, the mice treated with the *miR-1-3p* agomir showed gut bacterial penetration into the inner mucus layer according to FISH [Figure 4F; Supplementary Figure 4G], and this effect was accompanied by high permeability to FITC-dextran [Figure 4G], indicating a 'leaky gut'. Notably, microbiota dysbiosis [Figure 4H; Supplementary Figure 4H] mirrored previous observations in IBD, especially the enrichment of facultative anaerobes such as *Escherichia coli*,[16] illustrating the potential role of *miR-1-3p* in an imbalanced intestinal microenvironment. Moreover, compared with control mice, the mice with high *miR-1-3p* expression exhibited augmented expression levels of inflammatory genes [*TNF-α*, *IL-1β*, and *IL-6*] in the distal mucosa and liver [Supplementary Figure 4I], suggesting that the intestinal homeostasis imbalance in

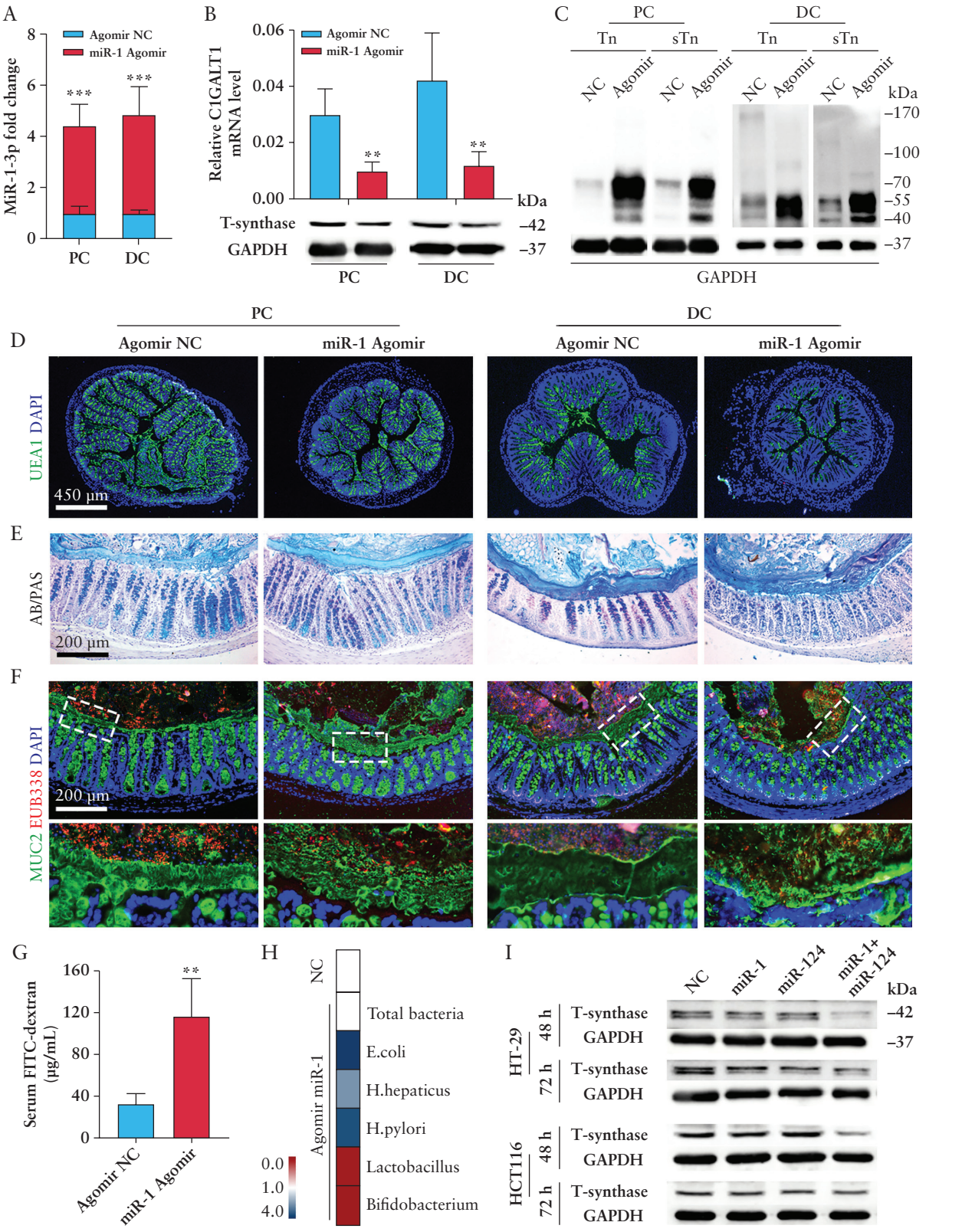

Figure 4. Mice overexpressing *miR-1-3p* show aberrant *O*-glycan induced mucus layer defects. A–C] High *miR-1-3p* expression [A], low T-synthase gene and protein expression [B], and high Tn and sTn expression [C] in the proximal and distal colonic mucosal tissues of *miR-1-3p* agomir-treated mice. D] Fluorescence images showing aberrant *O*-glycans in colonic mucosa with high *miR-1-3p* expression by using UEA1 staining. E] Representative AB/PAS staining of colonic tissues from the high *miR-1-3p* expression and control groups showing no differences in mucus thickness between the two groups. F] FISH using the EUB338 probe and mucin 2 antibody on mouse colon sections showing bacterial penetration into the inner mucus layer after *miR-1-3p* agomir administration. The magnified images show the boxed regions in greater detail. G] Intestinal hyperpermeability in *miR-1-3p* agomir-treated mice. H] Microbiota dysbiosis in distal

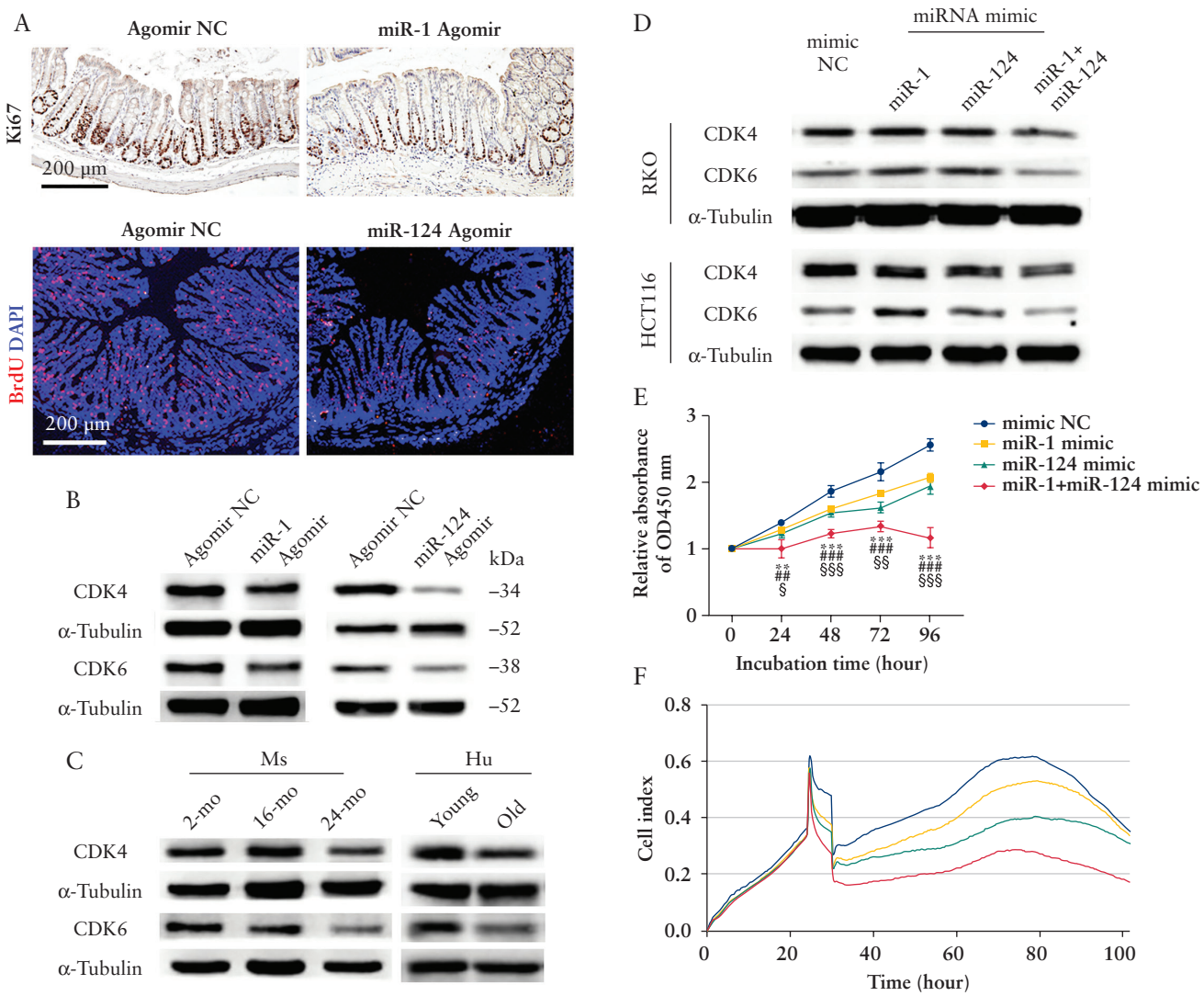

Figure 5. *MiR-1-3p* and *miR-124-3p* synergistically impair epithelial cell proliferation by inhibiting CDK4/6 expression. A] Immunohistological staining of Ki67 and immunofluorescent staining of BrdU showing a decrease in the number of proliferating cells in the distal colon of agomir-treated mice. B, C] Low expression of CDK4 and CDK6 in agomir-treated mice [B], ageing mice, and elderly people [C]. D] *MiR-1-3p* and *miR-124-3p* synergistically downregulated CDK4/6 protein expression in cells. E, F] RKO cell growth was monitored using CCK-8 [E] and RTCA [F] assays in control and mimic-treated cells. Data are presented as mean ± SD; ***p* <0.01, ****p* <0.001 compared with mimic NC group; ##*p* <0.01, ###*p* <0.001 compared with *miR-1-3p* mimic group; §*p* <0.05, §§ *p*<0.01, §§§*p* <0.001 compared with *miR-124-3p* mimic group [ANOVA and LSD tests]. *n* = 3 repeats for CCK-8 and RTCA assay. Ms, mouse; Hu, human; SD, standard deviation.

miR-1-3p overexpressing mice potentially contributes to a systemic proinflammatory response. Of greater interest are the very similar expression patterns of *miR-1-3p* and *miR-124-3p* and their effects on T-synthase expression.[12] We further demonstrated that these two miRNAs had a synergistic inhibitory effect on T-synthase expression [Figure 4I; Supplementary Figure 4J]. HT-29 and HCT116 cells were transiently transfected with full-dose *miR-1-3p* mimic, full-dose *miR-124-3p* mimic, or half-dose *miR-1-3p* mimic combined with half-dose *miR-124-3p* mimic. The results showed that compared with the control group, the single transfected groups and the group cotransfected with *miR-1-3p* and *miR-124-3p* exhibited significantly decreased T-synthase expression levels at 72 h, but only the cotransfected cells displayed reduced T-synthase expression at 48 h, illustrating that the T-synthase level decreased earlier and more sharply in the cotransfection group than in the single transfection groups.

3.5 *MiR-1-3p* and *miR-124-3p* have synergistic inhibitory effects on epithelial cell proliferation

In addition to mucus barrier breakdown, slow epithelial cell renewal was observed in old mice [Figure 1H]. *MiR-206*, a member of the miR-1 family, and *miR-124-3p* have been demonstrated to induce a decrease in cell proliferation by downregulating CDK4 and CDK6 expression.[17–20] We thus investigated the biological roles of *miR-1-3p*

colonic mucosal tissues of *miR-1-3p* agomir-treated mice. I] *MiR-1-3p* and *miR-124-3p* synergistically downregulated T-synthase protein expression in cells; the T-synthase level decreased earlier and more sharply in the cotransfection group than in the single-transfection group. Data are presented as mean ± SD; ***p* <0.01, ****p* <0.001 compared with agomir NC group [Student's t test]. *n* = 5 mice per group. PC, proximal colon; DC, distal colon; MUC2, mucin 2; SD, standard deviation; FISH, fluorescence *in situ* hybridisation; NC, negative control.

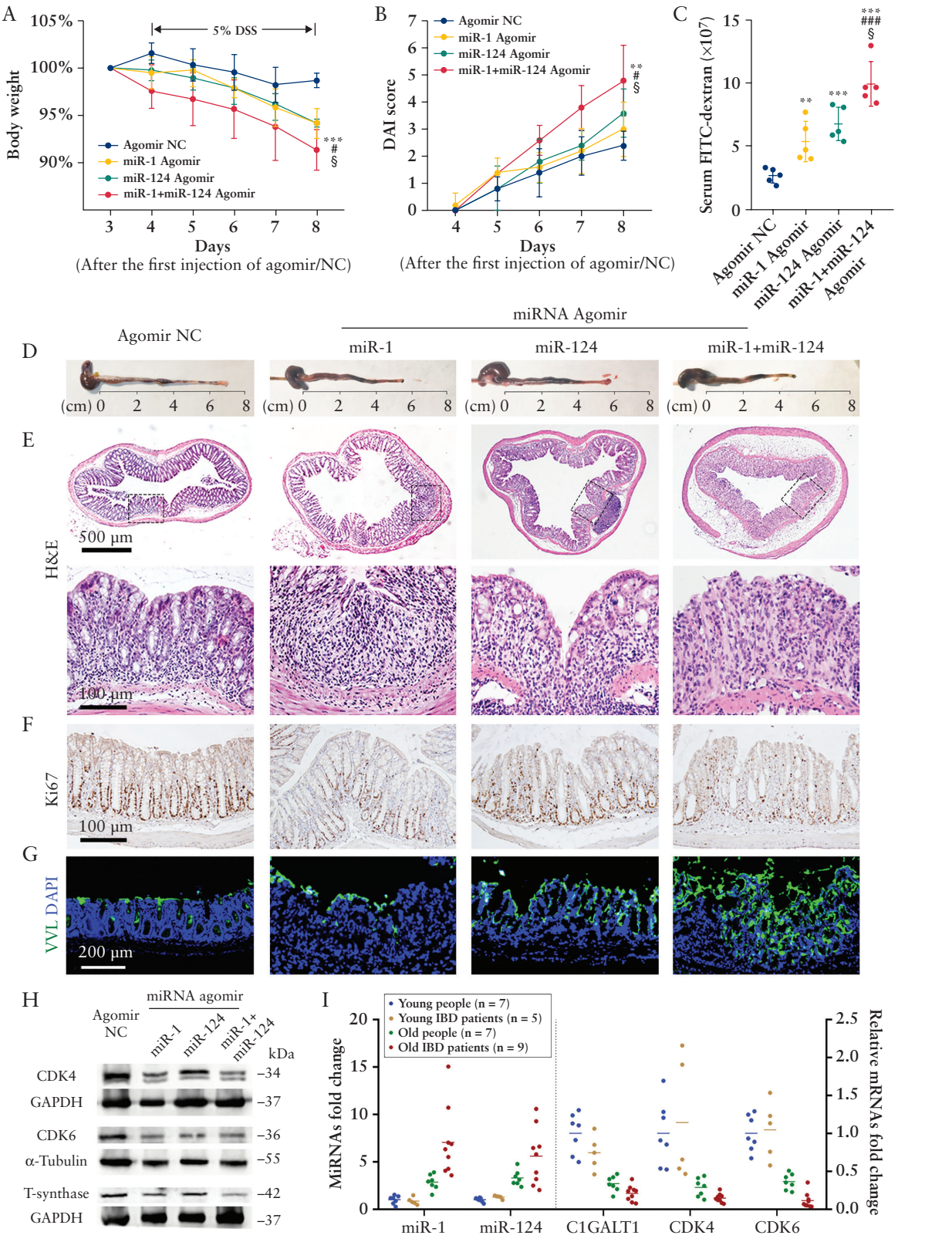

Figure 6. *MiR-1-3p* and *miR-124-3p* synergistically exacerbate DSS-induced colitis and are increased in elderly IBD patients. A, B] Greater reduction in body weight [A] and increase in DAI score [B] in mice treated with the combination of agomirs targeting both miRNAs after DSS administration. C] Intestinal hyperpermeability in agomir-treated mice detected by measuring serum FITC-dextran levels. D] Representative gross morphology of the mouse colon. E, F, G] Representative H&E images [E], immunostaining of Ki67 [F], and fluorescence images of VVL [G] in mouse distal colons. H] Low CDK4/6 and T-synthase expression in distal colonic mucosal tissues of agomir-treated mice. Data are presented as mean ± SD; $^{**}p$ <0.01, $^{***}p$ <0.001 compared with agomir NC group; #p <0.05, ###p <0.001 compared with *miR-1-3p* agomir group; §p <0.05, §§p <0.01 compared with *miR-124-3p* agomir group [ANOVA and LSD tests]. n = 5 mice per group. I] Scatter plot graph showing high expression of *miR-1-3p* and *miR-124-3p* and low expression of *C1GALT1*, *CDK4*, and *CDK6* in mucosal biopsies of the distal colon from elderly IBD patients using real-time qPCR. SD, standard deviation; DSS, dextran sulphate sodium; DAI, disease activity index; H&E, haematoxylin and eosin; IBD, inflammatory bowel disease; PCR, polymerase chain reaction; NC, negative control.

and *miR-124-3p* in enterocytes by analysing the pan-proliferation marker Ki67 and BrdU by immunohistology and immunofluorescence, respectively, in the colons of agomir-treated mice. Consistent with the increased expression of *miR-1-3p* [Figure 4A] and *miR-124-3p*,[12] reduced numbers of Ki67- and BrdU-positive cells were observed within the crypts of the distal colon of agomir-treated young mice [Figure 5A; Supplementary Figure 5A, B, available as Supplementary data at *ECCO-JCC* online]. Additionally, in accordance with the diminished proliferative ability, the *miR-1-3p*/*miR-124-3p* agomir-treated population showed attenuated CDK4/6 expression [Figure 5B; Supplementary Figure 5C, D], and these results were consistent with those in mucosal tissues from older individuals [Figure 5C; Supplementary Figure 5E, F]. Given that *miR-1-3p* and *miR-124-3p* downregulate CDK4/6 expression, we also examined the synergistic inhibitory effect of these two miRNAs on proliferation. RKO and HCT116 cells were transfected with *miR-1-3p* and *miR-124-3p* mimic alone or together. Compared with the control, the cotransfection group showed a sharp decrease in CDK4/6 expression level [Figure 5D; Supplementary Figure 5G, H]. Similarly, *in vitro* treatment with *miR-1-3p* and/or *miR-124-3p* mimic resulted in suppression of RKO [Figure 5E, F] and HCT116 [Supplementary Figure 5I, J] cell proliferation, especially in the cotransfection group, as determined by CCK-8 assay and real-time cell analyser [RTCA] experiments. Therefore, the data provide evidence that the cotransfection of *miR-1-3p* and *miR-124-3p* downregulates CDK4/6 expression and synergistically inhibits epithelial cell proliferation.

3.6. Mice overexpressing *miR-1-3p* and *miR-124-3p* show more severe DSS-induced colitis

Our previous study indicated that the *miR-124-3p* induced defects in the mucus barrier increase the susceptibility to colitis.[12] Here, we observed strong collaboration between *miR-1-3p* and *miR-124-3p* in enteritis. Young mice [2 mo] were injected with *miR-1-3p* and *miR-124-3p* agomir alone or together [each at a half-dose] and then treated with DSS to induce colitis [Supplementary Figures 1A, 6A, available as Supplementary data at *ECCO-JCC* online]. Compared with the mice injected with a single miRNA agomir, those injected with two miRNA agomirs were more susceptible to acute DSS-induced colitis and had much worse colonic injury. This injury was characterised by greater body weight loss [Figure 6A], a higher disease activity index [DAI] score [Figure 6B], greater gut permeability to FITC-dextran [Figure 6C], and a heavier spleen [Supplementary Figure 6B] in cotreated mice than in single miRNA-treated mice, but there was no significant difference among groups in colon length [Figure 6D; Supplementary Figure 6C]. We further found that co-injected mice developed severe colitis with higher colonic histopathology damage scores [Figure 6E; Supplementary Figure 6D], confirming superficial inflammation. Consistent with this finding, the proliferative ability of epithelial cells in the co-injected mice was markedly decreased [Figure 6F; Supplementary Figure 6E]. In addition, the distal colonic mucosa from the co-injection group exhibited a tendency toward lower T-synthase expression and more Tn/sTn accumulation, indicating miRNA-induced aberrant *O*-glycosylation [Figure 6G; Supplementary Figure 6F]. These results were associated with reduced CDK4, CDK6, and T-synthase protein levels and elevated Tn and sTn protein levels [Figure 6H; Supplementary Figure 6G, H, I]. These data suggested that the combination of *miR-1-3p* and *miR-124-3p* in enterocytes markedly exacerbated DSS-induced colitis. Furthermore, *miR-1-3p* and *miR-124-3p* that increased in the elderly had shown higher expression in elderly IBD patients compared with young IBD samples. Combined with decreased *C1GALT1* and *CDK4/6* in elderly IBD patients, these results supported the contribution of two miRNAs in IBD progression during ageing and partly explained why elder people often suffer from a relatively high risk of developing IBD [Figure 6I; Supplementary Figure 6J–M].

4 Discussion

IBD is an idiopathic disease and a focus of GI research. A variety of factors have been implicated in the complex pathogenesis of IBD. It is generally thought that the intestinal barrier changes with ageing, becoming an important individual contributing factor for IBD in the elderly population.[11,21] Our study showed that intestinal permeability increases with age, adding to the evidence for the 'leaky gut' during ageing.[11] An elegant study showed that intestinal barrier dysfunction is correlated with the lifespan of *Drosophila* and is a more accurate predictor of age-onset mortality than chronological age,[22] which makes research on the ageing intestinal barrier more meaningful.

Substantial research has shown that the intestinal epithelial apical junctional complex, which includes tight junctions and adherens junctions, contributes to intestinal barrier function via its role in regulating paracellular permeability.[23,24] In this study, intercellular junction proteins, such as claudin-1, claudin-3, ZO-1, occludin, and E-cadherin, were downregulated in the epithelium of the distal colon in 24-mo old mice, whereas claudin-2 expression was upregulated, indicating that the hyperpermeability in aged mice was at least partially due to abnormal epithelial microstructure.

Furthermore, increased IEC proliferation contributes to enhanced intestinal epithelial barrier function.[25,26] We discovered that colon epithelial cells from older individuals exhibited decreased growth compared with those from young individuals; this decreased growth will prolong the exposure to bacteria and other harmful metabolites, partially contributing to the disrupted intestinal homeostasis. In fact, changes in IEC proliferation in elderly individuals are somewhat controversial. Moorefield *et al.*[27] showed increased intestinal epithelial stem cell [IESC] proliferation with age, which might lead to increased DNA damage, resulting in p53-activated IESC apoptosis and decreased IESC function. However, Powell *et al.*[28] stated that a decline in colonic epithelial cell proliferation is not evident in geriatric mice. Another study found that p16 restraint of CDK activation is sufficient to inhibit IEC proliferation, resulting in the characteristics of ageing in somatic tissues of mammals.[29] Regardless, the intestinal epithelium is central to maintaining the peaceful coexistence of dietary components and commensals, controlling mucosal immunological homeostasis and defending against potentially harmful pathogens, and these cells are continuously replenished by multipotent IESCs residing in intestinal crypts.[30,31] Deficient IEC proliferation is obviously detrimental for the long-term maintenance of GI microstructure and function.

Previous studies have elucidated that CDK4 and CDK6, the proven target mRNAs of *miR-206*,[17,18] promote cell cycle entry via formation of the CDK4/6-cyclin D complex.[32] *MiR-206* shares identical seed sequences with *miR-1-3p*,[33] allowing us to focus on *miR-1-3p*, which was identified in the high-throughput analysis. In our study, *miR-1-3p* exhibited the same regional expression pattern and expression trend as *miR-124-3p*, which we have reported on previously.[12] Coincidentally, CDK4/6 expression can also be regulated by *miR-124-3p*.[19,20] Practically, our *in vitro* and *in vivo* findings did indeed point to an miRNA-induced decrease in the proliferative ability of cells that expressed high levels of *miR-1-3p* and *miR-124-3p* due to the downregulation of CDK4/6 expression, and these phenomena

closely resemble the observations made in colons of older individuals. Furthermore, the combination of *miR-1-3p* and *miR-124-3p* had a synergistic effect on CDK4/6. RKO and HCT116 cells were transfected with *miR-1-3p* and *miR-124-3p* mimics, alone or in combination. Compared with the group treated with *miR-1-3p* or *miR-124-3p* alone, the cotransfection group exhibited lower CDK4/6 protein expression, revealing that the combination of these miRNAs has the potential to synergistically suppress epithelial cell proliferation. Most extraordinarily, elevated *miR-1-3p* and *miR-124-3p* levels were observed in the mice at 16 mo, whereas a profound decrease in the proliferative capacity of epithelial cells was observed at 24 mo but not at 16 mo. We hypothesised that, as an important factor for maintaining epithelial function and intestinal homeostasis, the renewal of the epithelium is controlled by diverse genes and multistep processes and that *miR-1-3p*/*miR-124-3p* may only play a partial role in regulating proliferation. Many issues remain to be studied in the future.

Although a substantial number of studies have shown that intestinal tight junction barrier dysfunction can accelerate the onset and severity of colitis,[34] and this dysfunction has been recognised as a major aetiological factor in IBD, the roles of intestinal epithelial glycosylation in homeostasis and gut microbiota interactions in IBD have received increasing attention.[35] We observed a deficiency in mucin-type *O*-glycosylation in the distal colon beginning at 16 mo, before the disruption in epithelial microstructure and decrease in proliferation. Our data raised the intriguing possibility that damage to the mucus barrier, rather than disruption of the mucosal architecture, might be a contributing factor that results in epithelial hyperpermeability at the beginning of ageing [at approximately 50 years]. The normally impenetrable inner colon mucus layer is formed by sheets of mucin 2 that separate bacteria from the epithelium. The *O*-glycosylation of mucin 2 is critical and relies on the rate-limiting glycosyltransferase T-synthase.[36,37] The development of spontaneous colitis in mucin 2-deficient mice[38,39] and IL-10 deficient mice[40] confirmed the protective properties of the inner colonic mucus layer, suggesting that a decline in mucus barrier function might occur before colitis onset. Our results[12] showed that the loss of T-synthase and reduced mucin glycosylation appeared beginning at 16 mo and became prominent at 24 mo. The changes in mucus properties and the subsequently increased microbiota-epithelial contact in the distal colon led to disturbances in the mucosal immune system and inflammation, which can trigger the development of intestinal inflammatory diseases. Hence, improving the properties of colonic mucus would be an effective strategy to delay GI ageing and ameliorate early age-related inflammatory symptoms in the clinic. In this study, *miR-1-3p* was confirmed to directly downregulate *C1GALT1* expression and impair the intestinal mucus barrier function via decreased T-synthase-related mucin *O*-glycosylation. Intriguingly, all the age-related changes in *miR-1-3p* expression were observed exclusively in the distal colon, which was consistent with the distinct regional expression pattern of *miR-124-3p*/T-synthase we previously reported.[12] Furthermore, we found that *miR-1-3p* and *miR-124-3p* exerted a synergistic inhibitory effect on T-synthase, indicating that these two miRNAs are endogenous cooperative factors that regulate dynamic changes in gut mucus by modulating *O*-glycosylation in ageing people.

Normally, ageing is universal and results in mild or moderate changes in the expression of a range of miRNAs throughout the body rather than the severe abnormal expression of a single miRNA. Given the elevated levels of *miR-1-3p* and *miR-124-3p* during ageing and their robust functional roles in inhibiting T-synthase and CDK4/6 expression, we expanded our study by inducing DSS colitis in miRNA agomir-pretreated mice. Compared with high-dose agomir treatment targeting a single miRNA, the co-administration of low doses of two miRNAs exacerbated colitis after DSS treatment, indicating that slightly elevated *miR-1-3p* and *miR-124-3p* expression during ageing significantly increases the susceptibility to inflammation. Combined with our results that *miR-1-3p* and *miR-124-3p* were upregulated in colonic mucosa biopsies of old IBD patients, these findings support *miR-1-3p* and *miR-124-3p* as attractive targets to achieve multitarget and high-efficiency regulatory effects for the management of IBD in the geriatric population. Interestingly, miRNAs that belong to the same miRNA cluster and family are often thought to have close functional relationships and to co-regulate or coordinately regulate multiple biological processes. For instance, Zhao *et al.*[41] reported that *miR-524-3p* and *miR-524-5p* exerted a synergistic inhibitory effect on glioma cells. Pencheva *et al.*[42] revealed a convergent and cooperative multi-miRNA network including *miR-1908*, *miR-199a-5p*, and *miR-199a-3p*, which drove melanoma metastasis. The miR-23~27~24 clusters regulate multiple aspects of T cell biology.[43] However, *miR-1-3p* and *miR-124-3p* are not members of the same gene cluster/family, and we suspect that these molecules are unsaturated in our body and exert synergistic effects by binding to different sites of *C1GALT1*, *CDK4*, and *CDK6* in the same cell or different cells. The exact mechanism underlying this synergistic effect has yet to be investigated.

In *Drosophila*, gut dysfunction appears to be a primary driver of ageing and mortality, and the intestine represents a potentially important target for interventions that promote longevity.[44–46] The identification of the determinants that delay ageing in the human body has proven to be more challenging. In the present study, *miR-1-3p* and *miR-124-3p*, which exhibit slightly elevated expression in the ageing colon, work together in both goblet cells and IECs to disrupt the intestinal barrier by changing mucus properties and suppressing epithelial cell proliferation, supporting their crucial synergistic role in accelerating GI ageing and enhancing susceptibility to colitis. The cooperation between these miRNAs is a new feature of key regulators involved in the onset and progression of colitis in elderly populations. Although the manifestations of ageing are a feature of later life, their underlying molecular bases certainly begin earlier. Our discovery provides a possible effective or optimal time window for intervention and a new research direction for postponing the course of GI ageing in the future.

The high-throughput data used in the study are publicly available at the NCBI Gene Expression Omnibus under the accession number GSE174837 and GSE175493. The data underlying this article are available in the article and in its online supplementary material.

Funding

This work was supported by Beijing Natural Science Foundation [grant number 5202007], National Natural Science Foundation of China [grant numbers 31801011, 31771332, 32071180], and Support Project of High-level Teachers in Beijing Municipal Universities in the Period of 13th Five-year Plan [IDHT20170516].

Conflict of Interest

The authors declare that they have no conflict of interest.

Author Contributions

T-yS and D-sZ designed the project, analysed the data and wrote the manuscript. T-yS, Y-qL, F-qZ, and YG performed the experiments. H-mS, BW, and SY contributed reagents/materials/analysis tools. F-qJ helped draft the manuscript. All authors approved the final manuscript.

Supplementary Data

Supplementary data are available online at *ECCO-JCC* online.

References

1. Kaplan GG. The global burden of IBD: from 2015 to 2025. *Nat Rev Gastroenterol Hepatol* 2015;**12**:720–7.
2. Kaplan GG, Windsor JW. The four epidemiological stages in the global evolution of inflammatory bowel disease. *Nat Rev Gastroenterol Hepatol* 2021;**18**:56–66.
3. Ha CY, Katz S. Clinical implications of ageing for the management of IBD. *Nat Rev Gastroenterol Hepatol* 2014;**11**:128–38.
4. Singh S, Picardo S, Seow CH. Management of inflammatory bowel diseases in special populations: obese, old, or obstetric. *Clin Gastroenterol Hepatol* 2020;**18**:1367–80.
5. Sartor RB, Wu GD. Roles for intestinal bacteria, viruses, and fungi in pathogenesis of inflammatory bowel diseases and therapeutic approaches. *Gastroenterology* 2017;**152**:327–39.e4.
6. Shin W, Kim HJ. Intestinal barrier dysfunction orchestrates the onset of inflammatory host-microbiome cross-talk in a human gut inflammation-on-a-chip. *Proc Natl Acad Sci U S A* 2018;**115**:E10539–47.
7. Chopyk DM, Grakoui A. Contribution of the intestinal microbiome and gut barrier to hepatic disorders. *Gastroenterology* 2020;**159**:849–63.
8. Martini E, Krug SM, Siegmund B, Neurath MF, Becker C. Mend your fences: the epithelial barrier and its relationship with mucosal immunity in inflammatory bowel disease. *Cell Mol Gastroenterol Hepatol* 2017;**4**:33–46.
9. Mehandru S, Colombel JF. The intestinal barrier, an arbitrator turned provocateur in IBD. *Nat Rev Gastroenterol Hepatol* 2021;**18**:83–4.
10. López-Otín C, Kroemer G. Hallmarks of Health. *Cell* 2021;**184**:33–63.
11. Branca JJV, Gulisano M, Nicoletti C. Intestinal epithelial barrier functions in ageing. *Ageing Res Rev* 2019;**54**:100938.
12. Huang L, Sun TY, Hu LJ, *et al*. Elevated miR-124-3p in the ageing colon disrupts mucus barrier and increases susceptibility to colitis by targeting T-synthase. *Ageing Cell* 2020;**19**:e13252.
13. Kalla R, Ventham NT, Kennedy NA, *et al*. MicroRNAs: new players in IBD. *Gut* 2015;**64**:504–17.
14. Xuan Y, Yang H, Zhao L, *et al*. MicroRNAs in colorectal cancer: small molecules with big functions. *Cancer Lett* 2015;**360**:89–105.
15. Flurkey K. *The Jackson Laboratory Handbook on Genetically Standardized Mice*. 6th edn. Bar Harbor, ME: Jackson Laboratory; 2009.
16. Lloyd-Price J, Arze C, Ananthakrishnan AN, *et al*.; IBDMDB Investigators. Multi-omics of the gut microbial ecosystem in inflammatory bowel diseases. *Nature* 2019;**569**:655–62.
17. Xiao H, Xiao W, Cao J, *et al*. miR-206 functions as a novel cell cycle regulator and tumor suppressor in clear-cell renal cell carcinoma. *Cancer Lett* 2016;**374**:107–16.
18. Wu H, Tao J, Li X, *et al*. MicroRNA-206 prevents the pathogenesis of hepatocellular carcinoma by modulating expression of met proto-oncogene and cyclin-dependent kinase 6 in mice. *Hepatology* 2017;**66**:1952–67.
19. Deng X, Ma L, Wu M, *et al*. miR-124 radiosensitizes human glioma cells by targeting CDK4. *J Neurooncol* 2013;**114**:263–74.
20. Pierson J, Hostager B, Fan R, Vibhakar R. Regulation of cyclin dependent kinase 6 by microRNA 124 in medulloblastoma. *J Neurooncol* 2008;**90**:1–7.
21. Ahmadi S, Wang S, Nagpal R, *et al*. A human-origin probiotic cocktail ameliorates ageing-related leaky gut and inflammation via modulating the microbiota/taurine/tight junction axis. *JCI Insight* 2020;**5**:e132055.
22. Rera M, Clark RI, Walker DW. Intestinal barrier dysfunction links metabolic and inflammatory markers of aging to death in Drosophila. *Proc Natl Acad Sci U S A* 2012;**109**:21528–33.
23. Otani T, Furuse M. Tight junction structure and function revisited. *Trends Cell Biol* 2020;**30**:805–17.
24. Buckley A, Turner JR. Cell biology of tight junction barrier regulation and mucosal disease. *Cold Spring Harb Perspect Biol* 2018;**10**:a029314.
25. Liu L, Yao J, Li Z, *et al*. miR-381-3p knockdown improves intestinal epithelial proliferation and barrier function after intestinal ischemia/reperfusion injury by targeting nurr1. *Cell Death Dis* 2018;**9**:411.
26. Bär F, Bochmann W, Widok A, *et al*. Mitochondrial gene polymorphisms that protect mice from colitis. *Gastroenterology* 2013;**145**:1055–63.e3.
27. Moorefield EC, Andres SF, Blue RE, *et al*. Aging effects on intestinal homeostasis associated with expansion and dysfunction of intestinal epithelial stem cells. *Aging [Albany NY]* 2017;**9**:1898–915.
28. Powell DN, Swimm A, Sonowal R, *et al*. Indoles from the commensal microbiota act via the AHR and IL-10 to tune the cellular composition of the colonic epithelium during aging. *Proc Natl Acad Sci U S A* 2020;**117**:21519–26.
29. Boquoi A, Arora S, Chen T, Litwin S, Koh J, Enders GH. Reversible cell cycle inhibition and premature ageing features imposed by conditional expression of p16Ink4a. *Ageing Cell* 2015;**14**:139–47.
30. Peterson LW, Artis D. Intestinal epithelial cells: regulators of barrier function and immune homeostasis. *Nat Rev Immunol* 2014;**14**:141–53.
31. Allaire JM, Crowley SM, Law HT, Chang SY, Ko HJ, Vallance BA. The intestinal epithelium: central coordinator of mucosal immunity. *Trends Immunol* 2018;**39**:677–96.
32. The I, Ruijtenberg S, Bouchet BP, *et al*. Rb and FZR1/Cdh1 determine CDK4/6-cyclin D requirement in C. elegans and human cancer cells. *Nat Commun* 2015;**6**:5906.
33. Lin CY, Lee HC, Fu CY, *et al*. MiR-1 and miR-206 target different genes to have opposing roles during angiogenesis in zebrafish embryos. *Nat Commun* 2013;**4**:2829.
34. Odenwald MA, Turner JR. The intestinal epithelial barrier: a therapeutic target? *Nat Rev Gastroenterol Hepatol* 2017;**14**:9–21.
35. Kudelka MR, Stowell SR, Cummings RD, Neish AS. Intestinal epithelial glycosylation in homeostasis and gut microbiota interactions in IBD. *Nat Rev Gastroenterol Hepatol* 2020;**17**:597–617.
36. Ju T, Brewer K, D'Souza A, Cummings RD, Canfield WM. Cloning and expression of human core 1 beta1,3-galactosyltransferase. *J Biol Chem* 2002;**277**:178–86.
37. Xia L, Ju T, Westmuckett A, *et al*. Defective angiogenesis and fatal embryonic hemorrhage in mice lacking core 1-derived O-glycans. *J Cell Biol* 2004;**164**:451–9.
38. Johansson ME, Phillipson M, Petersson J, Velcich A, Holm L, Hansson GC. The inner of the two Muc2 mucin-dependent mucus layers in colon is devoid of bacteria. *Proc Natl Acad Sci U S A* 2008;**105**:15064–9.
39. Van der Sluis M, De Koning BA, De Bruijn AC, *et al*. Muc2-deficient mice spontaneously develop colitis, indicating that MUC2 is critical for colonic protection. *Gastroenterology* 2006;**131**:117–29.
40. Johansson ME, Gustafsson JK, Holmén-Larsson J, *et al*. Bacteria penetrate the normally impenetrable inner colon mucus layer in both murine colitis models and patients with ulcerative colitis. *Gut* 2014;**63**:281–91.
41. Zhao K, Wang Q, Wang Y, *et al*. EGFR/c-myc axis regulates TGFβ/Hippo/Notch pathway via epigenetic silencing miR-524 in gliomas. *Cancer Lett* 2017;**406**:12–21.
42. Pencheva N, Tran H, Buss C, *et al*. Convergent multi-miRNA targeting of ApoE drives LRP1/LRP8-dependent melanoma metastasis and angiogenesis. *Cell* 2012;**151**:1068–82.
43. Cho S, Wu CJ, Yasuda T, *et al*. miR-23~27~24 clusters control effector T cell differentiation and function. *J Exp Med* 2016;**213**:235–49.
44. Biteau B, Hochmuth CE, Jasper H. JNK activity in somatic stem cells causes loss of tissue homeostasis in the ageing Drosophila gut. *Cell Stem Cell* 2008;**3**:442–55.
45. Clark RI, Salazar A, Yamada R, *et al*. Distinct shifts in microbiota composition during Drosophila ageing impair intestinal function and drive mortality. *Cell Rep* 2015;**12**:1656–67.
46. Rera M, Azizi MJ, Walker DW. Organ-specific mediation of lifespan extension: more than a gut feeling? *Ageing Res Rev* 2013;**12**:436–44.